Scientia Pharmaceutica

Österreichische Pharmazeutische Gesellschaft

MDPI

Article

Synthesis and Analgesic Activity of Cridanimod–Monoterpene Conjugates

Danil D. Anikev [1,2], Anastasia Yu. Filippova [1], Olga I. Yarovaya [1,3,*], Serafim A. Tishchenko [1,2], Alla V. Pavlova [1], Alina A. Sonina [1], Kseniya S. Kovaleva [1], Mikhail V. Khvostov [1,3], Tatyana G. Tolstikova [1], Andrey Yu. Petrov [4] and Nariman F. Salakhutdinov [1]

[1] Department of Medicinal Chemistry, N.N. Vorozhtsov Novosibirsk Institute of Organic Chemistry of Siberian Branch of RAS, 630090 Novosibirsk, Russia; d.anikev@g.nsu.ru (D.D.A.); filippova@nioch.nsc.ru (A.Y.F.); s.tishchenko@g.nsu.ru (S.A.T.); pavlova@nioch.nsc.ru (A.V.P.); belalina04@nioch.nsc.ru (A.A.S.); kseniya.kovaleva3103@yandex.ru (K.S.K.); khvostov@nioch.nsc.ru (M.V.K.); tolstiktg@nioch.nsc.ru (T.G.T.); anvar@nioch.nsc.ru (N.F.S.)

[2] Department of Natural Sciences, Novosibirsk State University, 630090 Novosibirsk, Russia

[3] Institute of Medicine and Medical Technologies, Novosibirsk State University, 630090 Novosibirsk, Russia

[4] Department of Biomedical and Translational Research FSBI Scientific Advisory Center of Toxicology Named After S.N. Golikova FMBA of Russia, St. Bekhtereva 1, 192019 St. Petersburg, Russia; adanol@mail.ru

* Correspondence: ooo@nioch.nsc.ru

Abstract

Cridanimod (acridoneacetic acid), the active ingredient of the immunomodulatory drug Cycloferon®, has a well-characterized antiviral profile, but an unexplored analgesic potential. Bornane monoterpenes, notably (+)-camphor and (−)-fenchone, are established scaffolds for analgesic drug design. We therefore synthesized thirteen cridanimod–monoterpene conjugates—seven amides, three acylhydrazones, and three esters—by EDCI/DMAP-mediated coupling or CDI/DBU-promoted esterification, and evaluated them in mice at an oral dose of 10.0 mg/kg in the acetic acid writhing and hot plate tests, with diclofenac sodium (10.0 mg/kg) as the reference. Acridoneacetic acid and Cycloferon® were themselves inactive in both assays. By contrast, six of the thirteen conjugates were significantly active ($p < 0.05$) in at least one test, with distinct leads in each: amide **19** matched diclofenac in the writhing test (−63.7% vs. −64.4%), whereas acylhydrazone **23** exceeded diclofenac in the hot plate test (+43.9% vs. +25.7%). The divergent profiles suggest that different structural subclasses engage peripheral and central antinociceptive mechanisms. Conjugation thus converts an analgesically inactive immunomodulator into a substance yielding analgesics that match or exceed a standard NSAID at the same oral dose, providing a promising starting point for the development of new pain-relieving agents.

Keywords: cridanimod; acridoneacetic acid; Cycloferon®; monoterpenes; camphor; fenchone; analgesic activity; writhing test; hot plate test; structure–activity relationship

Academic Editor: Thierry Besson

Received: 30 June 2026
Revised: 27 July 2026
Accepted: 29 July 2026
Published: 31 July 2026

1. Introduction

Pain remains one of the most prevalent and debilitating medical conditions worldwide, affecting hundreds of millions of people and imposing enormous social and economic burdens on healthcare systems [1]. Despite the availability of numerous analgesic agents, ranging from non-steroidal anti-inflammatory drugs (NSAIDs) to opioids, the management of chronic and acute pain continues to pose significant clinical challenges due to issues of insufficient efficacy, gastrointestinal toxicity [2], dependence, and other adverse

effects [3]. The need for novel analgesic products with improved safety profiles and distinct mechanisms of action therefore remains a priority in medicinal chemistry.

Cridanimod (acridoneacetic acid, 9-oxo-10(9*H*)-acridineacetic acid) is a low-molecular-weight synthetic compound that has attracted considerable attention as a multifunctional pharmacological agent [4,5]. As an immunomodulatory drug, cridanimod triggers the production of interferons, which play a central role in the immune response against viral infections, and is therefore primarily used in the treatment and prevention of various viral infections, including influenza, acute respiratory viral infections, HIV, and herpes [4,6]. Its meglumine salt, marketed as Cycloferon®, is a clinically approved interferon inducer that has been widely used in Russia and other countries [6,7]. Mechanistically, in murine systems, acridoneacetic acid activates the innate immune STING–TBK1–IRF3 signaling pathway [8], while recent studies have also revealed direct antiviral activity against SARS-CoV-2 that appears to be independent of interferon induction [5,9]. Beyond these antiviral and immunomodulatory effects, the broad biological profile of acridoneacetic acid encompasses antitumor and, importantly for the present study, anti-inflammatory activity [4]—a property that suggests a possible link to pain modulation, since inflammation is a major contributor to nociception in both acute and chronic pain states. To our knowledge, however, the analgesic potential of acridoneacetic acid itself has not been systematically explored, and chemical modification of its framework therefore represents a rational and largely untapped strategy for the discovery of new bioactive compounds with potentially expanded therapeutic applications.

Terpenoids constitute the largest and most structurally diverse class of natural products, with tens of thousands of known structures, and represent a rich source of biologically active scaffolds for drug discovery [10]. Within this family, monoterpenoids built on the bornane skeleton—most notably camphor, fenchone, and their derivatives—have been extensively studied by our group and others as pharmacophoric building blocks for antiviral, analgesic, and other biologically active compounds [10,11]. The rigid, enantiopure bicyclic framework of bornane confers favorable steric properties and contributes to high target-binding affinity and selectivity. Importantly, multiple bornane-type compounds and their amine, alcohol, and hydrazone derivatives have independently demonstrated analgesic activity in standard in vivo nociception models [12,13], making them attractive starting fragments for the design of new analgesics.

Molecular hybridization, in which two pharmacophoric fragments are combined within a single molecular framework, has emerged as a powerful strategy in medicinal chemistry [14]. Such conjugates allow simultaneous modulation of pharmacokinetic properties, target affinity, and biological activity, and have been successfully applied in the development of antiviral, anticancer, and anti-inflammatory agents, particularly when natural-product fragments are merged with bioactive heterocyclic scaffolds [15]. In this context, conjugating the acridoneacetic acid core with monoterpenoid fragments offers a rational approach toward the discovery of novel bioactive molecules with potential analgesic activity, drawing simultaneously on the anti-inflammatory profile of the heterocyclic core and on the established antinociceptive activity of the bornane fragments.

We hypothesized that linking the acridoneacetic acid core to bornane-type monoterpenoid fragments would yield new bioactive entities with measurable antinociceptive activity, despite the parent acridoneacetic acid not being known for such effects. To test this hypothesis, we designed and synthesized a focused library of thirteen cridanimod–monoterpene conjugates featuring three different linker types—amide, ester, and acylhydrazone (Scheme 1). The starting amines, alcohols, and hydrazones were drawn from four sources: (+)-camphor and (−)-fenchone, used as precursors to the corresponding primary amines (bornylamine and fenchylamine) and ketone-derived hydrazones; commercially

available (−)-borneol and (+)-fenchol as the alcohol building blocks; ketopinic acid, providing access to amines bearing additional functional groups on the bornane skeleton; and non-terpenoid cyclohexanone-derived counterparts (cyclohexylamine, cyclohexanol, and cyclohexanone hydrazone), included in each series as controls to gauge the specific contribution of the bicyclic bornane framework. The analgesic activity of all synthesized compounds was then evaluated in vivo in mice using the acetic acid writhing test and the hot plate test, with diclofenac sodium as the reference drug.

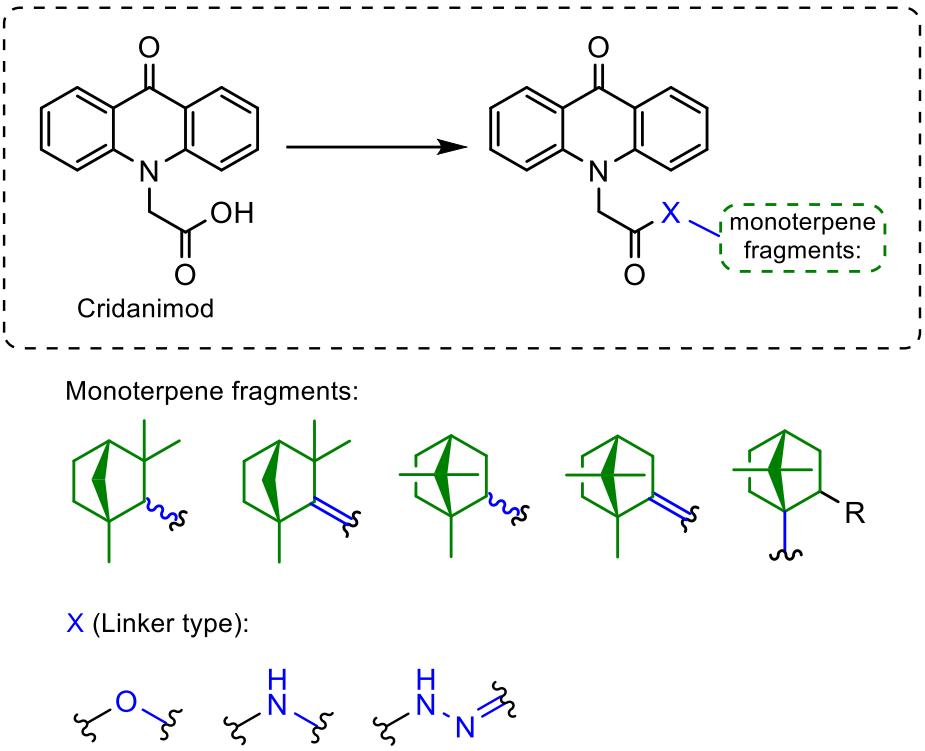

Scheme 1. General scheme of acridoneacetic acid modification.

2. Materials and Methods

2.1. Chemistry

2.1.1. General Procedure

^{1}H and ^{13}C NMR spectra were recorded on Bruker spectrometers (Bruker BioSpin GmbH, Ettlingen, Germany), including an AV-300 instrument at 300.13 MHz (^{1}H) and 75.47 MHz (^{13}C), an AV-400 instrument at 400.13 MHz (^{1}H) and 100.61 MHz (^{13}C), and a DRX-500 instrument at 500.13 MHz (^{1}H) and 125.76 MHz (^{13}C) in $CDCl_3$; chemical shifts δ were reported in ppm relative to residual $CHCl_3$ [d($CHCl_3$) 7.26, d($CDCl_3$) 77.16 ppm], J in Hz. The atom numbering in the compounds is given for the assignment of the NMR spectra signals and does not match the atom numbering in the nomenclature name. High-resolution mass spectra were recorded on DFS Thermo Scientific (Waltham, MA, USA) and Agilent 7200 Accurate Mass Q-TOF spectrometers (Agilent Tech., Santa Clara, CA, USA) in full scan mode in the range m/z 0–500, electron impact ionization 70 eV at direct sample input.

Separation and isolation of the reaction products was carried out using silica gel column chromatography (60–200 μm, Macherey-Nagel, Düren, Germany). Thin layer chromatography was performed on Merck silica gel (60 F254) TLC plates and visualized under a 254 nm UV lamp. All reagents and other chemicals were purchased from Across, Merck, ABCR and TCI and used without further purification.

2.1.2. Synthesis of Cridanimod Amides (Compound **14**–**20**)

To a stirred solution of the corresponding amine **1–4** (0.395 mmol, 1.0 equiv) and DMAP (0.02 mmol, 0.05 equiv) in anhydrous dichloromethane (20 mL per 1 mmol of acid) at room temperature was added acridoneacetic acid (0.395 mmol, 1.0 equiv) in one portion. EDCI (0.513 mmol, 1.3 equiv) was then added in one portion, and the resulting reaction mixture was stirred at room temperature for 12–18 h (reaction progress monitored by TLC).

After completion, the reaction mixture was successively washed with 10% aqueous citric acid, water, saturated aqueous Na_2CO_3, and brine. The organic layer was dried over anhydrous Na_2SO_4, filtered, and concentrated under reduced pressure. The crude product was purified by column chromatography on silica gel ($CHCl_3$) to afford the corresponding acridoneacetic acid amides **14**–**20** as individual compounds.

2-(9-Oxoacridin-10(9*H*)-yl)-*N*-((1*R*,2*R*,4*S*)-1,3,3-trimethylbicyclo[2.2.1]heptan-2-yl)acetamide (**14**). The compound was obtained as a light green powder in 62% yield, m.p. 235.7–239.1 °C. ^{1}H NMR (500 MHz, $CDCl_3$) δ 8.58–8.51 (*m*, 2H, H-18, H-25), 7.73 (*ddd*, *J* = 8.8, 7.0, 1.6 Hz, 2H, H-20, H-23), 7.41–7.31 (*m*, 4H, H-19, H-21, H-22, H-24), 5.81 (*d*, *J* = 9.6 Hz, 1H, NH), 5.05–4.93 (*m*, 2H, 2–12), 3.62 (*dd*, *J* = 9.7, 1.9 Hz, 1H, H-6), 1.32–1.15 (*m*, 4H, H-2′, H-3″, H-4, H-7′), 1.08 (*dd*, *J* = 10.3, 1.6 Hz, 1H, H-7″), 1.04 (*s*, 3H, H-10), 0.84 (*s*, 3H, H-8), 0.81–0.69 (*m*, 1H, H-3′), 0.37 (*s*, 3H, H-9). ^{13}C NMR (126 MHz, $CDCl_3$) δ 178.04 (C-17), 167.24 (C-11), 141.91 (C-13, C-14), 134.58 (C-20, C-23), 128.26 (C-18, C-25), 122.70 (C-15, C-16), 122.61 (C-19, C-24), 114.52 (C-21, C-22), 63.21 (C-6), 51.31 (C-12), 48.45 (C-1), 47.84 (C-4), 42.36 (C-7), 39.17 (C-5), 30.83 (C-10), 26.74 (C-2), 25.61 (C-3), 21.14 (C-9), 19.44 (C-8). HRMS (EI) *m*/*z* calculated for $C_{25}H_{28}O_2N_2$ $[M]^{+\bullet}$ 388.2145, found 388.2140.

2-(9-Oxoacridin-10(9*H*)-yl)-*N*-((1*R*,2*R*,4*R*)-1,7,7-trimethylbicyclo[2.2.1]heptan-2-yl)acetamide (**15**). The compound was obtained as a light green powder in 75% yield, m.p. 253.8–257.6 °C. ^{1}H NMR (400 MHz, $CDCl_3$) δ 8.58 (*dd*, 2H, H-18, H-25), 7.76 (*ddd*, *J* = 1.7, 7.0, 8.7 Hz, 2H, H-20, H-23), 7.42–7.33 (*m*, 4H, H-19, H-21, H-22, H-24), 5.72 (*d*, *J* = 9.2 Hz, 1H, NH), 4.96 (*s*, 2H, H-12), 3.87 (*td*, *J* = 4.6, 9.1 Hz, 1H, H-6), 1.75 (*dd*, *J* = 9.0, 13.5 Hz, 1H, H-5″), 1.65–1.47 (*m*, 2H, H-2″, H-4), 1.52–1.40 (*m*, 1H, H-3″), 1.28–1.15 (*m*, 3H, H-2′, H-5′), 1.11–0.99 (*m*, 1H, H-3′), 0.58 (*s*, 3H, H-9), 0.50 (*s*, 3H, H-8), 0.05 (*s*, 3H, H-10). ^{13}C NMR (126 MHz, $CDCl_3$) δ 178.28 (C-17), 167.81 (C-11), 141.59 (C-13, C-14), 133.76 (C-20, C-23), 128.38 (C-18, C-25), 122.65 (C-19, C-24), 122.01 (C-15, C-16), 114.47 (C-21, C-22), 64.45 (C-6), 48.77 (C-1), 47.16 (C-4), 41.22 (C-7), 39.56 (C-5), 29.99 (C-10), 26.55 (C-2), 25.61 (C-3), 21.41 (C-9), 19.47 (C-8). HRMS (EI) *m*/*z* calculated for $C_{25}H_{28}O_2N_2$ $[M]^{+\bullet}$ 388.2149, found 388.2140.

2-(9-Oxoacridin-10(9*H*)-yl)-*N*-((1*R*,2*S*,4*R*)-1,7,7-trimethylbicyclo[2.2.1]heptan-2-yl)acetamide (**16**). The compound was obtained as a light green powder in 84% yield, m.p. 264.9–266.2 °C. ^{1}H NMR (500 MHz, $CDCl_3$) δ 8.47–8.43 (*m*, 2H, H-18, H-25), 7.77–7.72 (*m*, 2H, H-20, H-23), 7.39–7.35 (*m*, 2H, H-21, H-22), 7.34–7.29 (*m*, 2H, H-19, H-14), 5.07 (*d*, *J* = 9.1 Hz, 1H, NH), 5.02–4.92 (*m*, 2H, H-12), 4.35–4.28 (*m*, 1H, H-6), 2.30–2.22 (*m*, 1H, H-5″), 1.54–1.45 (*m*, 2H, H-4, H-3″), 1.12–1.02 (*m*, 1H, H-2″), 0.90 (*s*, 3H, H-2′, H-3′), 0.76 (*s*, 3H, H-9), 0.75–0.70 (*m*, 2H, H-8), 0.73 (*s*, 3H, H-10), 0.61–0.55 (*m*, 1H, H-5′). ^{13}C NMR (126 MHz, $CDCl_3$) δ 178.04 (C-17), 167.01 (C-11), 142.17 (C-13, C-14), 134.59 (C-20, C-23), 128.16 (C-18, C-25), 122.75 (C-19, C-24), 122.56 (C-15, C-16), 114.51 (C-21, C-22), 54.02 (C-6), 51.65 (C-12), 49.73 (C-1), 48.22 (C-7), 44.72 (C-4), 37.15 (C-5), 28.01 (C-3), 27.65 (C-2), 19.76 (C-8), 18.68 (C-9), 13.88 (C-10). HRMS (EI) *m*/*z* calculated for $C_{25}H_{28}O_2N_2$ $[M]^{+\bullet}$ 388.2145, found 388.2138.

N-((1*S*,4*R*)-7,7-dimethyl-2-oxobicyclo[2.2.1]heptan-1-yl)-2-(9-oxoacridin-10(9*H*)-yl)acetamide (**17**). The compound was obtained as a light yellow powder in 42% yield, m.p. 253.1–259.6 °C. ^{1}H NMR (500 MHz, $CDCl_3$) δ 8.58–8.53 (*m*, 2H, H-17, H-24), 7.76–7.70 (*m*, 2H, H-19, H-22), 7.40–7.31 (*m*, 4H, H-18, H-20, H-21, H-23), 6.27 (*s*, 1H, NH), 5.03–4.92 (*m*, 2H, H-11), 3.15–3.05 (*m*, 1H, H-6″), 2.35–2.27 (*m*, 1H, H-3″), 2.19–2.10 (*m*, 1H, H-5″), 2.02 (*t*, *J* = 4.5 Hz,

1H, H-4), 1.94 (*d*, *J* = 18.7 Hz, 1H, H-3′), 1.48–1.39 (*m*, 2H, H-5′, H-6′), 1.18 (*s*, 3H, H-9), 0.65 (*s*, 3H, H-8). ^{13}C NMR (126 MHz, $CDCl_3$) *δ* 212.65 (C-2), 178.21 (C-16), 167.57 (C-10), 142.27 (C-12, C-13), 134.47 (C-19, C-22), 128.23 (C-17, C-24), 122.86 (C-14, C-15), 122.39 (C-18, C-23), 114.42 (C-20, C-21), 73.02 (C-1), 51.76 (C-11), 48.56 (C-7), 41.25 (C-3), 40.51 (C-4), 26.71 (C-5), 22.55 (C-6), 21.39 (C-9), 19.28 (C-8). HRMS (EI) *m*/*z* calculated for $C_{24}H_{24}O_3N_2$ $[M]^{+\bullet}$ 388.1781, found 388.1780.

N-((1*S*,2*R*,4*R*)-2-hydroxy-7,7-dimethylbicyclo[2.2.1]heptan-1-yl)-2-(9-oxoacridin-10(9*H*)-yl)acetamide (**18**). The compound was obtained as a white powder in 84% yield, m.p. 262.5–262.9 °C. ^{1}H NMR (500 MHz, $CDCl_3$) *δ* 8.59–8.55 (*m*, 2H, H-17, H-24), 7.79–7.74 (*m*, 2H, H-19, H-22), 7.45–7.34 (*m*, 4H, H-18, H-20, H-21, H-23), 5.85 (*s*, 1H, NH), 5.03–4.93 (*m*, 2H, H-11), 4.34–4.29 (*m*, 1H, H-2), 2.82 (*m*, 1H, OH), 1.85–1.76 (*m*, 2H, H-3″, H-6″), 1.73–1.58 (*m*, 4H, H-3′, H-4, H-5″, H-6′), 1.16–1.10 (*m*, 1H, H-5′), 0.69 (*s*, 3H, H-9), 0.48 (*s*, 3H, H-8). ^{13}C NMR (126 MHz, $CDCl_3$) *δ* 178.09 (C-16), 167.97 (C-10), 141.96 (C-12, C-13), 134.74 (C-19, C-22), 128.34 (C-17, C-24), 122.78 (C-14, C-15), 122.68 (C-18, C-23), 114.41 (C-20, C-21), 75.01 (C-2), 67.18 (C-1), 51.66 (C-11), 47.10 (C-7), 41.79 (C-4), 39.38 (C-3), 30.35 (C-6), 27.03 (C-5), 20.07 (C-8), 19.23 (C-9). HRMS (EI) *m*/*z* calculated for $C_{24}H_{26}O_3N_2$ $[M]^{+\bullet}$ 390.1938, found 390.1936.

N-((1*R*,4*R*)-7,7-Dimethylbicyclo[2.2.1]heptan-1-yl)-2-(9-oxoacridin-10(9*H*)-yl)acetamide (**19**). The compound was obtained as a light green powder in 77% yield, m.p. 246.3–249.2 °C. ^{1}H NMR (300 MHz, $CDCl_3$) *δ* 8.63–8.53 (*m*, 2H, H-17, H-24), 7.81–7.71 (*m*, 2H, H-19, H-22), 7.44–7.32 (*m*, 4H, H-18, H-20, H-21, H-23), 5.61 (*s*, 1H, NH), 4.91 (*s*, 2H, H-11), 2.19–2.06 (*m*, 2H, H-2″, H-6″), 1.81–1.56 (*m*, 4H, H-2′, H-3″, H-5″, H-6′), 1.56–1.49 (*m*, 1H, H-4), 1.34–1.20 (*m*, 2H, H-3′, H-5′), 0.47 (*m*, 6H, H-8, H-9). ^{13}C NMR (75 MHz, $CDCl_3$) *δ* 178.06 (C-16), 167.28 (C-10), 141.96 (C-12, C-13), 134.65 (C-19, C-22), 128.30 (C-17, C-24), 122.77 (C-14, C-15), 122.58 (C-18, C-23), 114.45 (C-20, C-21), 64.03 (C-1), 51.66 (C-11), 47.51 (C-7), 42.54 (C-4), 32.89 (C-2, C-6), 28.05 (C-3, C-5), 18.61 (C-8, C-9). HRMS (EI) *m*/*z* calculated for $C_{24}H_{26}O_2N_2$ $[M]^{+\bullet}$ 374.1989, found 374.1986.

N-Cyclohexyl-2-(9-oxoacridin-10(9*H*)-yl)acetamide (**20**). The compound was obtained as a light yellow powder in 79% yield, m.p. 268.0–269.9 °C. ^{1}H NMR (500 MHz, MeOD, $CDCl_3$) *δ* 8.53–8.41 (*dd*, *J* = 8.0, 1.7 Hz, 2H, H-14, H-21), 7.81–7.74 (*ddd*, *J* = 8.7, 7.0, 1.8 Hz, 2H, H-15, H-20), 7.51–7.41 (*d*, *J* = 8.7 Hz, 2H, H-17, H-18), 7.40–7.29 (*t*, *J* = 7.5 Hz, 2H, H-16, H-19), 5.08–5.02 (*s*, 2H, H-8), 3.83–3.73 (*m*, 1H, H-6), 1.97–1.84 (*m*, 2H, H-1″, H-5″), 1.79–1.69 (*m*, 2H, H-2′, H-4′), 1.68–1.55 (*m*, 1H), 1.44–1.05 (*m*, 6H, H-1′, H-2″, H-3, H-4″, H-5′). ^{13}C NMR (126 MHz, MeOD + $CDCl_3$) *δ* 179.59 (C-13), 167.42 (C-7), 143.31 (C-9, C-10), 135.04 (C-16, C-19), 127.78 (C-14, C-21), 122.65 (C-11, C-12), 122.52 (C-15, C-20), 115.47 (C-17, C-18), 50.39 (C-8), 49.42 (C-6), 33.06 (C-1, C-5), 30.10, 25.79 (C-3), 25.39 (C-2, C-4). HRMS (EI) *m*/*z* calculated for $C_{21}H_{22}O_2N_2$ $[M]^{+\bullet}$ 334.1676, found 334.1670.

2.1.3. Synthesis of Cridanimod Acylhydrazones (Compound **21**–**23**)

To a stirred solution of the corresponding hydrazone **1**–**4** (0.395 mmol, 1.0 equiv) and DMAP (0.05 mmol, 0.05 equiv) in anhydrous dichloromethane (20 mL per 1 mmol of acid) at room temperature was added acridoneacetic acid (0.395 mmol, 1.0 equiv) in one portion. EDCI (0.513 mmol, 1.3 equiv) was then added in one portion, and the resulting reaction mixture was stirred at room temperature for 12–18 h (reaction progress monitored by TLC).

After completion, the reaction mixture was successively washed with 10% aqueous citric acid, water, saturated aqueous Na_2CO_3, and brine. The organic layer was dried over anhydrous Na_2SO_4, filtered, and concentrated under reduced pressure. The crude product was purified by column chromatography on silica gel ($CHCl_3$) to afford the corresponding acridoneacetic aciylhydrazones **21**–**23** as individual compounds. When required, the reactions were carried out under an inert atmosphere using dry solvents.

2-(9-Oxoacridin-10(9*H*)-yl)-*N*′-((1*R*,4*S*,*Z*)-1,3,3-trimethylbicyclo[2.2.1]heptan-2-ylidene) acetohydrazide (**21**). The compound was obtained as a white powder in 82% yield, m.p. 259.2–264.7 °C. ^{1}H NMR (400 MHz, $CDCl_3$) δ 8.97–8.93 (*s*, 1H, NH), 8.60–8.50 (*td*, *J* = 7.7, 1.7 Hz, 2H, H-18, H-25), 7.78–7.62 (*ddd*, *J* = 8.7, 6.9, 1.7 Hz, 2H, H-20, H-23), 7.48–7.26 (*m*, 4H, H-19, H-21, H-22, H-24), 5.51–5.37, 5.13–5.03 (*s*, 2H, H-12), 1.91–1.86 (*m*, 1H, H-4), 1.84–1.53 (*m*, 4H, H-2′, H-3′, H-3″), 1.52–1.37 (*m*, 3H, H-2″, H-7), 1.31–1.20 (*m*, 6H, H-8, H-10), 1.18–1.11 (*s*, 3H, H-9). ^{13}C NMR (101 MHz, $CDCl_3$) δ 178.44, 177.75 (C-17), 170.81 (C-11), 168.61 (C-6), 142.83, 141.59 (C-13, C-14), 134.94, 133.93 (C-20, C-23), 128.38, 127.85 (C-18, C-25), 122.73 (C-15, C-16), 121.57 (C-19, C-24), 114.87, 114.47 (C-21, C-22), 51.76 (C-1), 50.31 (C-5), 49.86 (C-4), 47.90, 47.66 (C-12), 42.97, 42.68 (C-7), 34.35 (C-2), 25.08, 24.79 (C-3), 23.13 (C-9), 22.78 (C-8), 17.27 (C-10). HRMS (EI) *m*/*z* calculated for $C_{25}H_{27}O_2N_3$ $[M]^{+\bullet}$ 401.2098, found 401.2093.

2-(9-Oxoacridin-10(9*H*)-yl)-*N*′-((1*R*,4*R*,*E*)-1,7,7-trimethylbicyclo[2.2.1]heptan-2-ylidene) acetohydrazide (**22**). The compound was obtained as a white powder in 86% yield, m.p. 219.6–222.2 °C. ^{1}H NMR (500 MHz, $CDCl_3$) δ 9.61 (*s*, 1H, NH), 8.57 (*dd*, *J* = 8.0, 1.7 Hz, 2H, H-18, H-25), 7.68 (*ddd*, *J* = 8.7, 6.9, 1.7 Hz, 2H, H-20, H-23), 7.36 (*d*, *J* = 8.7 Hz, 2H, H-21, H-22), 7.30 (*t*, *J* = 7.5 Hz, 1H, H-19, H-24), 5.47 (*d*, *J* = 5.0 Hz, 2H, H-12), 2.11–2.02 (*m*, 1H, H-5″), 1.85–1.67 (*m*, 3H, H-2, H-3″), 1.58 (*d*, *J* = 17.4 Hz, 1H, H-5′), 1.36 (*ddd*, *J* = 13.0, 9.3, 3.6 Hz, 1H, H-4), 1.31–1.20 (*m*, 0H, H-3′), 1.00 (*s*, 3H, H-8), 0.91 (*s*, 3H, H-10), 0.70 (*s*, 3H, H-9). ^{13}C NMR (126 MHz, DMSO) δ 178.47 (C-17), 169.18 (C-11), 169.06 (C-6), 142.80 (C-13, C-14), 133.94 (C-20, C-23), 127.91 (C-18, C-25), 122.67 (C-15, C-16), 121.62 (C-19, C-24), 114.84 (C-21, C-22), 53.03 (C-1), 48.10 (C-12), 47.69 (C-7), 43.86 (C-4), 33.88 (C-5), 32.63 (C-2), 27.15 (C-3), 19.64 (C-9), 18.69 (C-8), 11.24 (C-10). HRMS (EI) *m*/*z* calculated for $C_{25}H_{27}O_2N_3$ $[M]^{+\bullet}$ 401.2098, found 401.2103.

N′-Cyclohexylidene-2-(9-oxoacridin-10(9*H*)-yl)acetohydrazide (**23**). The compound was obtained as a light yellow powder in 85% yield, m.p. 262.3–262.7 °C. ^{1}H NMR (500 MHz, DMSO-d_6) δ 10.96 (s, 0.6H, NH), 10.84 (s, 0.4H, NH), 8.35 (d, *J* = 7.6 Hz, 2H, H-14, H-21), 7.84–7.76 (m, 2H, H-16, H-19), 7.65 (d, *J* = 8.9 Hz, 1H, H-17, H-18), 7.56 (d, *J* = 8.8 Hz, 1H), 7.38–7.31 (m, 2H, H-15, H-20), 5.58 (s, 1H), 5.32 (s, 1H, H-8), 2.50–2.45 (m, 2H, H-1, H-5), 2.30 (dt, *J* = 35.1, 6.2 Hz, 2H), 1.76–1.52 (m, 6H, H-2, H-3, H-4). ^{13}C NMR (126 MHz, DMSO-d_6) δ 176.84 (C-13), 168.66 (C-7), 163.77, 161.81 (C-6), 157.63, 142.56 (C-9, C-10), 134.25 (C-16, C-19), 126.62 (C-14, C-21), 121.60 (C-11, C-12), 121.49 (C-15, C-20), 116.01 (C-17, C-18), 47.50 (C-8), 35.31, 35.04 (C-1, C-5), 26.99 (C-2, C-4), 25.80, 25.20 (C-3). HRMS (EI) *m*/*z* calculated for $C_{21}H_{21}O_2N_3$ $[M]^{+\bullet}$ 347.1628, found 347.1626.

2.1.4. Synthesis of Cridanimod Esters (Compound **24**–**26**)

N,*N*′-Carbonyldiimidazole (1.97 mmol, 1.0 equiv) was added portionwise to a solution of cridanimod (1.97 mmol, 1.0 equiv) in anhydrous DMF (15–20 mL per 1 mmol) under an argon atmosphere. The reaction mixture was stirred at 40 °C for 1 h to allow complete formation of the corresponding acyl imidazolide.

DBU (1.97 mmol, 1.0 equiv) was then added to the activated solution. Upon addition of DBU, the reaction mixture immediately turned dark orange. The corresponding alcohol (3.95 mmol, 2.0 equiv) was subsequently added, and the mixture was stirred at 40 °C for 24 h under argon. After addition of the alcohol, the initially dark orange solution gradually faded over several hours, becoming pale yellow. The progressive discoloration of the reaction mixture served as a convenient visual indicator of reaction progress (TLC control was additionally performed).

After completion, the reaction mixture was cooled to room temperature and diluted with diethyl ether. The organic phase was washed successively with 10% aqueous HCl, water, and 10% aqueous K_2CO_3. The organic layer was dried over anhydrous Na_2SO_4,

filtered, and concentrated under reduced pressure. The crude product was purified by column chromatography on silica gel using chloroform as eluent to afford the corresponding cridanimod esters **24**–**26** as individual compounds.

(1*R*,2*R*,4*S*)-1,3,3-Trimethylbicyclo[2.2.1]heptan-2-yl 2-(9-oxoacridin-10(9*H*)-yl)acetate (**24**). The compound was obtained as a white powder in 79% yield, m.p. 150.8–151.9 °C. **^{1}H NMR** (500 MHz, $CDCl_3$) δ 8.57 (dd, *J* = 8.0, 1.7 Hz, 2H, H-18, H-25), 7.75–7.68 (*m*, 2H, H-20, H-23), 7.40–7.29 (*m*, 4H, H-19, H-21, H-22, H-24), 5.18–5.06 (*m*, 2H, H-12, H-12′′), 4.43 (*d*, *J* = 2.0 Hz, 1H, H-6), 1.64 (*d*, *J* = 3.9 Hz, 1H, H-3′), 1.54–1.47 (*m*, 1H, H-4), 1.44–1.35 (*m*, 1H, H-2′′), 1.34–1.23 (*m*, 1H, H-3′′), 1.13–1.07 (*m*, 2H, H-2′, H-7′), 1.05 (*s*, 3H, H-10), 0.86 (*s*, 3H, H-8), 0.81 (*tt*, *J* = 12.5, 2.7 Hz, 1H, H-7′′), 0.59 (*s*, 3H, H-9). ^{13}C NMR (126 MHz, $CDCl_3$) *δ* 178.29 (C-17), 168.82 (C-11), 142.27 (C-13, C-14), 134.17 (C-20, C-23), 128.16 (C-18, C-25), 122.64 (C-19, C-24), 122.02 (C-15, C-16), 114.37 (C-21, C-22), 88.47 (C-6), 48.37 (C-1), 48.16 (C-4), 41.22 (C-7), 39.59 (C-5), 29.67 (C-10), 26.25 (C-2), 25.62 (C-3), 20.41 (C-9), 19.27 (C-8). HRMS (EI) *m*/*z* calculated for $C_{25}H_{27}O_3N$ $[M]^{+\bullet}$ 389.1986, found 389.1988.

(1*R*,2*S*,4*R*)-1,7,7-Trimethylbicyclo[2.2.1]heptan-2-yl 2-(9-oxoacridin-10(9*H*)-yl)acetate (**25**). The compound was obtained as a white powder in 86% yield, m.p. 129.6–131.1 °C. **^{1}H NMR** (500 MHz, $CDCl_3$) δ 8.56 (dd, *J* = 8.0, 1.7 Hz, 2H, H-18, H-25), 7.71 (ddd, *J* = 8.7, 6.9, 1.7 Hz, 2H, H-20, H-23), 7.36–7.28 (*m*, 4H, H-19, H-21, H-22, H-24), 5.08 (*d*, *J* = 1.3 Hz, 2H, H-12), 5.01–4.94 (*m*, 1H, H-6), 2.34 (*ddt*, *J* = 13.8, 9.9, 4.0 Hz, 1H, H-5′′), 1.73–1.68 (*m*, 1H, H-4), 1.63–1.52 (*m*, 2H, H-2′′, H-3′), 1.29 (*ddd*, *J* = 13.3, 9.4, 4.2 Hz, 1H, H-3′′), 1.07–0.97 (*m*, 1H, H-5′), 0.89–0.83 (*m*, 1H, H-2′), 0.84 (*s*, 3H, H-10), 0.77 (*s*, 3H, H-9), 0.64 (*s*, 3H, H-8). ^{13}C NMR (126 MHz, $CDCl_3$) *δ* 178.30 (C-17), 168.69 (C-11), 142.32 (C-13, C-14), 134.17 (C-20, C-23), 128.11 (C-18, C-25), 122.65 (C-19, C-24), 121.98 (C-15, C-16), 114.26 (C-21, C-22), 82.13 (C-6), 48.90 (C-1), 48.61 (C-12), 47.93 (C-7), 44.77 (C-4), 36.81 (C-5), 27.85 (C-2), 26.82 (C-3), 18.87 (C-10), 13.43 (C-9). HRMS (EI) *m*/*z* calculated for $C_{25}H_{27}O_3N$ $[M]^{+\bullet}$ 389.1986, found 389.1983.

Cyclohexyl 2-(9-oxoacridin-10(9*H*)-yl)acetate (**26**). The compound was obtained as a light green powder in 82% yield, m.p. 179.2–179.3 °C. ^{1}H NMR (400 MHz, $CDCl_3$) *δ* 8.60–8.53 (*dd*, *J* = 8.1, 1.7 Hz, 2H, H-14, H-21), 7.74–7.67 (*ddd*, *J* = 8.7, 7.0, 1.7 Hz, 2H, H-16, H-19), 7.35–7.28 (*m*, 4H, H-15, H-17, H-18, H-20), 5.07–5.02 (*s*, 2H, H-8), 4.98–4.89 (*m*, 1H, H-6), 1.88–1.78 (*m*, 2H, H-1′′, H-5′′), 1.64–1.54 (*m*, 2H, H-2′, H-4′), 1.53–1.15 (*m*, 6H, H-2′′, H-3, H-4′′). ^{13}C NMR (101 MHz, $CDCl_3$) *δ* 178.32 (C-13), 167.85 (C-7), 142.45 (C-9, C-10), 134.15 (C-16, C-19), 128.08 (C-14, C-21), 122.76 (C-11, C-12), 121.94 (C-15, C-20), 114.36 (C-17, C-18), 74.88 (C-6), 48.84 (C-8), 31.49 (C-1, C-5), 25.23 (C-3), 23.48 (C-2, C-4). HRMS (EI) *m*/*z* calculated for $C_{21}H_{21}O_3N$ $[M]^{+\bullet}$ 335.1516, found 335.1517.

2.2. Biological Studies

2.2.1. Animals

All studies were carried out on non-breeding CD-1 albino mice (male) weighing 20–25 g, 8 animals in each group (SPF-vivarium of the Institute of Cytology and Genetics of the Siberian Branch of the Russian Academy of Sciences). Mice were maintained at 22–25 °C on a 12 h light-dark cycle with food and water available *ad libitum*.

The study protocol was approved by the Bioethics Commission of the Laboratory of Pharmacological Research, N.N. Vorozhtsov Novosibirsk Institute of Organic Chemistry, SB RAS (Protocol No. R-14-2026-04-01 dated 1 April 2026). All animal experiments were carried out in accordance with the guidelines laid down in the legislation of the Russian Federation and the European Union Directive of 22 September 2010 (2010/63/EU).

2.2.2. Analgesic Tests

Agents were dissolved in saline containing 0.5% Tween 80 just before use and were administered per os, 1 h before testing. Control group: saline was administered per os in blank mice (0.2 mL per 10 g of animal weight), 1 h before testing. Analgesic activity of test agents was assessed using the acetic acid-induced writhing test and hot plate test.

In the hot plate test, animals were placed individually on a metallic plate (VWR Hotplate/Stirrer 725-HPS, USA) warmed to 54 ± 0.5 °C until either licking of the hind paw or jumping [16]. This time of pain response was recorded by a stopwatch, and the animal was immediately taken away from the plate and put back into the cage. A 60 s cut-off time is assigned in this protocol. The percentage of protection (P) was calculated according to the following equation: Protection P (%) = 100%•(Kexp − Kcontrol)/Kcontrol, where Kcontrol is the mean time on the hot plate in the control group, and Kexp is the mean time on the hot plate in the test group.

In the acetic acid-induced writhing test, the pain reaction was determined by the number of abdominal convulsions, recorded from the 5th to the 8th min following the acetic acid injection (0.75%, 0.1 mL/10 g body weight) [17,18]. The percentage of inhibition of pain response (IPR) was calculated according to the following equation: Inhibition of pain response (IPR) = 100%•(Kcontrol − Kexp)/Kcontrol, where Kcontrol is the mean number of writhes in the control group, and Kexp is the mean number of writhes in the test group.

Statistical analysis was conducted in the Statistica 10.0 program using the Mann–Whitney U Test to assess the significance ($p < 0.05$) of differences. The data are presented in the format: mean ± standard error of the mean (SE).

2.3. In Silico Physicochemical and ADME Predictions

The structures of acridoneacetic acid and compounds 14–26 were prepared using LigPrep in Schrödinger Maestro 14.4 (Schrödinger, LLC, New York, NY, USA) with the OPLS4 force field. Ionization states were generated with Epik at pH 7.40 ± 2.00; the original state and specified stereochemistry were retained, salts were removed, and additional tautomers were not generated.

The LigPrep-prepared structures were analyzed using QikProp in standard mode. QPlogPo/w, QPlogS, QPlogBB, Caco-2/MDCK permeability, human oral absorption, PSA, HBD/HBA, and Lipinski Rule-of-Five violations were calculated. The complete descriptor set is provided in Table S1 (Supporting Information).

3. Results and Discussion

3.1. Chemistry

To evaluate how the linker nature and the monoterpene substitution affect analgesic activity, we designed a library of 13 cridanimod–monoterpene conjugates covering three connection types: amides (**14**–**20**), acylhydrazones (**21**–**23**), and esters (**24**–**26**) (Scheme 1). The starting amines, alcohols, and hydrazones were drawn from four distinct sources. First, (+)-camphor and (−)-fenchone served as precursors to bornylamine and fenchylamine (for amide formation) and to the corresponding hydrazones (for acylhydrazone formation). Second, commercially available (−)-borneol and (+)-fenchol were used directly as the alcohol building blocks for ester formation. Third, ketopinic acid provided access to amines **7**–**9** bearing additional functional groups at the bornane skeleton. Finally, non-terpenoid cyclohexanone-derived counterparts (cyclohexylamine, cyclohexanol, and cyclohexanone hydrazone) were included in each series as controls to gauge the specific contribution of the bicyclic bornane framework. Within the amide series, structural variation at the carbon bearing the nitrogen was explored: primary bornyl- and fenchyl-amines, amines

carrying an additional carbonyl or hydroxy group (derived from ketopinic acid), and the 7,7-dimethylnorbornyl-amine. A cyclohexyl counterpart was included in each series as a non-terpenoid control to gauge the specific contribution of the bicyclic bornane framework.

Synthesis of starting amines and hydrazones. Fenchylamine **4**, bornylamine **6**, amines **7–9**, and cyclohexylamine were selected as starting materials for the preparation of cridanimod amides. Commercially available fenchone was sequentially converted to oxime **1** and then to nitroimine **2** following reported procedures; treatment of the latter with gaseous ammonia in dry THF afforded imine **3**, which was subsequently reduced with sodium borohydride in methanol to give fenchylamine **4** with a predominance of the *endo*-isomer (*endo:exo* = 24:1). The second method involved reduction of oxime **1** with a nickel–aluminum alloy under alkaline conditions, affording a mixture of *endo*- and *exo*-isomers **4** in a 2:1 ratio. In the third approach, imine **3** was reduced with sodium cyanoborohydride in acidic medium (H_2SO_4), providing an isomer ratio of 2.6:1. In all cases, the reaction mixtures were analyzed by derivatization of the monoterpene amines with Boc_2O, followed by determination of the ratio of the obtained derivatives by GC/MS. The results of the reaction mixture analysis are presented in Scheme 2. Both the *exo*- and *endo*-isomers of bornylamine **6** were synthesized from (+)-camphor following reported procedures [19].

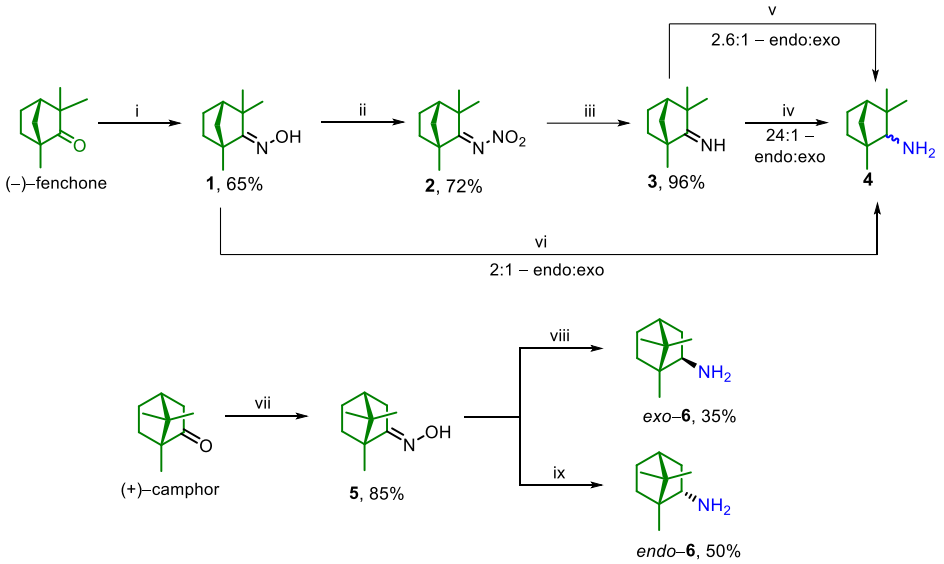

Scheme 2. Synthesis of fenchylamine and bornylamine. Reagents and conditions: (i): $NH_2OH{\cdot}HCl$, Et_3N, EtOH, reflux, 6 h; (ii): $NaNO_2$, H_2SO_4, Et_2O/H_2O, 16 h; (iii): NH_3 (gas), THF, 0 °C, 3 h; (iv): $NaBH_4$, MeOH, 4 h; (v): $NaBH_3CN$, AcOH, MeOH, 4 h; (vi): Ni-Al, KOH, THF, 2 h; (vii): $NH_2OH{\cdot}HCl$, Et_3N, EtOH, reflux, 6 h; (viii): $NaBH_4$, $NiCl_2{\cdot}6H_2O$, MeOH, −40 °C, 2 h; (ix): Ni/Al, NaOH, r.t., 3 h.

Amines **7–9** were prepared from a common starting material, following our previously established procedures [20] (Scheme 3). The synthesis starts with the two-step conversion of camphor-10-sulfonic acid **10** into ketopinic acid **11**. To obtain amine **7**, ketopinic acid **11** was first converted to the corresponding acid chloride and then to the acyl azide **12**, which was then subjected to Curtius rearrangement in refluxing toluene, followed by hydrolysis of the resulting isocyanate. Amine **8** was synthesized via the reduction of amine **7** using $NaBH_4$ in MeOH with $CeCl_3{\cdot}7H_2O$. Amine **9** was synthesized from ketopinic acid **11** via Wolff–Kishner reduction to acid **13**, followed by a Schmidt reaction.

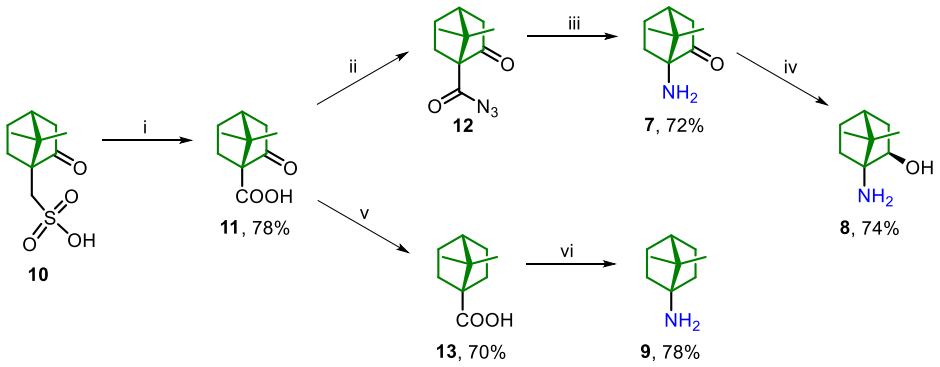

Scheme 3. Synthesis of amines **7**–**9**. Reagents and conditions: (i) (1) $SOCl_2$, reflux, 3 h, (2) $KMnO_4$, Na_2CO_3, 80 °C, 2 h; (ii) (1) $SOCl_2$, reflux, 3 h, (2) NaN_3, acetone/H_2O, 1 h; (iii) (1) toluene, reflux, 3 h, (2) H^+, reflux, 8 h; (iv) $NaBH_4$, $CeCl_3 \cdot 7H_2O$, MeOH, −30 °C, 4 h; (v) $N_2H_4 \cdot H_2O$, KOH, reflux, 8 h; (vi) H_2SO_4, NaN_3, 50 °C, 1 h.

Commercially available cyclohexylamine and cyclohexanol were used without further purification. Camphor and fenchone hydrazones were obtained by reaction of the corresponding ketones with hydrazine hydrate in ethanol. The structures of the obtained amines and hydrazones were confirmed by NMR spectroscopy and high-resolution mass spectrometry.

Screening of activation methods for acridoneacetic acid. Due to steric hindrance of the monoterpene substrates, activation of the carboxylic group of acridoneacetic acid proved non-trivial. Seven strategies were systematically examined using monoterpene amines, hydrazones, and alcohols prior to the preparation of the target conjugates (Table 1).

Table 1. Screening of activation methods for the reaction of acridoneacetic acid with monoterpene amines, hydrazones, and alcohols.

Entry	Activation Method	Reagents	Product Class	Outcome
1	Acyl chloride	$SOCl_2$	amides, acylhydrazones	Target products formed, accompanied by inseparable byproducts
2	Mixed anhydride	$ClCO_2Et$, Et_3N	amides, acylhydrazones	Mixed anhydride formed, but no conversion to target products
3	Uronium salt	HBTU, DIPEA	amides	No conversion of starting acid
4	Carbodiimide	DCC, DMAP	amides, acylhydrazones	Target amides were formed, but proved difficult to separate from *N*,*N*′-dicyclohexylurea.
5	Carbodiimide	EDCl, DMAP	amides, acylhydrazones	Clean couplings; esters not formed
6	Acyl imidazolide	CDI; CDI, Et_3N; CDI, DIPEA	esters	CDI reacted with the acid, but no substitution by the alcohol occurred
7	Acyl imidazolide	CDI, DBU	esters	Successful esterification

Four of the strategies proved unsuitable. Acyl chloride activation with $SOCl_2$ (entry 1) produced the target compounds but was consistently accompanied by significant amounts of inseparable byproducts, which precluded isolation of analytically pure material. Mixed-anhydride activation with ethyl chloroformate (entry 2) cleanly afforded the mixed-anhydride intermediate (confirmed by NMR monitoring), but no coupling to amines, hydrazones, or alcohols was observed under any of the conditions tested. HBTU in the presence of DIPEA (entry 3) did not activate acridoneacetic acid, with full recovery of the starting material. DCC/DMAP (entry 4) afforded the target amides, but the stoichiometric

N,*N*′-dicyclohexylurea byproduct co-eluted with the products on silica gel and could not be removed by chromatography.

Two protocols ultimately proved satisfactory. For amides and acylhydrazones, the water-soluble carbodiimide EDCl together with DMAP in anhydrous dichloromethane (entry 5) gave clean couplings; the EDCI-derived urea is water-soluble and is readily removed during aqueous workup. The same protocol, however, failed to promote esterification of the bornane-type alcohols, consistent with the low nucleophilicity of sterically hindered secondary alcohols toward carbodiimide-activated intermediates. For ester formation (entry 6), CDI activation in anhydrous DMF at 40 °C cleanly generated the acyl imidazolide intermediate; subsequent addition of the alcohol furnished the ester only in the presence of DBU (1.0 equiv), whereas Et_3N and DIPEA were ineffective under otherwise identical conditions. A distinctive fading of the deep orange color of the reaction mixture upon DBU addition served as a convenient visual indicator of reaction progress, complementing TLC monitoring.

Synthesis of the target cridanimod–monoterpene conjugates. With reliable activation protocols identified, the 13 target conjugates were assembled under the optimized conditions (Scheme 4). EDCI/DMAP-mediated coupling of acridoneacetic acid with amines **4**, **6**, **7–9**, and cyclohexylamine furnished the seven amides **14–20** in 42–84% isolated yield. Under the same conditions, condensation with the (+)-camphor, (−)-fenchone, and cyclohexanone-derived hydrazones delivered the three acylhydrazones **21–23** in 82–86% yield. Esters **24–26** were obtained from (−)-borneol, (+)-fenchol, and cyclohexanol, respectively, by CDI/DBU activation in DMF, in 79–86% yield. All target compounds were purified by silica gel column chromatography and characterized spectroscopically (see Section 2).

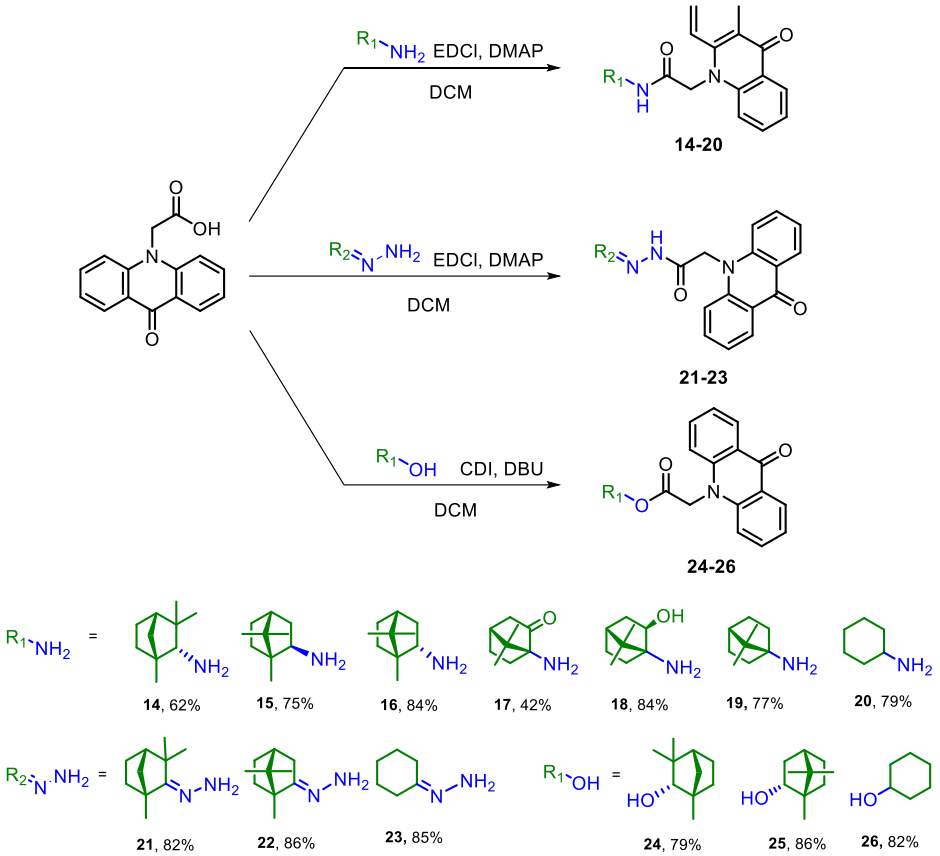

Scheme 4. General scheme of synthesis and structures of the obtained acridoneacetic acid derivatives.

3.2. Biology

The analgesic activity of acridoneacetic acid, Cycloferon®, and the obtained cridanimod–monoterpene conjugates **14–26** in a dose of 10.0 mg/kg (oral administration) was studied in the standard experimental pain models, namely the acetic acid-induced writhing (0.75% acetic acid, 0.1 mL for one animal, intraperitoneally) and hot plate (thermal stimulation, 54 ± 0.5 °C) tests. Sodium diclofenac in the same dose was used as a reference drug (Table 2). The acetic acid-induced writhing test is designed to evaluate acute visceral and deep somatic pain. Acetic acid induces chemical irritation and an inflammatory response in the abdominal cavity, with subsequent activation of nociceptors. The animals react with typical animal movements involving abdominal muscle contractions alternating with relaxation, extension of the hind limbs, and arching of the back, which is called writhing [21]. The hot plate test is employed to quantify the analgesic effect of test substances following thermal stimulation. In this test, the effect is assessed by the duration of presence of animals placed individually on a metallic plate warmed to 54.0 ± 0. 5 °C until either licking of the hind paw or jumping, which was recorded by a stopwatch [21].

Table 2. Analgesic activity and predicted physicochemical properties of acridoneacetic acid, Cycloferon®, compounds **14–26**, and sodium diclofenac (10.0 mg/kg dose).

Compound	Acetic Acid-Induced Writhing, *N*		Hot Plate, τ/*s*		Predicted ADME Properties		
	Control	Agent (IPR (%) [a])	Control	Agent (P (%) [b])	QPlogPo/w	QPlogS	QPPCaco, nm/s
Acridoneacetic acid	11.0 ± 2.2	8.9 ± 1.6	8.9 ± 1.2	10.3 ± 1.7	2.21	−2.54	133.0
Cycloferon®	11.0 ± 2.2	8.8 ± 1.6	8.9 ± 1.2	8.4 ± 1.3	—	—	—
14	9.2 ± 1.0	8.5 ± 1.4	8.7 ± 1.0	**14.1 ± 1.6** * (+62.1%)	4.23	−5.32	1898.4
15	10.8 ± 0.7	7.8 ± 1.9	12.1 ± 1.9	12.9 ± 1.8	4.18	−5.323	1718.9
16	11.3 ± 2.4	9.9 ± 2.0	9.8 ± 1.1	10.9 ± 1.1	4.07	−5.28	1572.9
17	10.8 ± 0.7	**6.6 ± 1.4** * (−38.9%)	12.1 ± 1.9	12.8 ± 0.9	3.29	−4.88	1003.3
18	11.3 ± 2.4	8.5 ± 2.1	9.8 ± 1.1	12.0 ± 1.3	3.04	−4.60	1041.9
19	11.3 ± 2.4	**4.1 ± 1.2** * (−63.7%)	9.8 ± 1.1	11.8 ± 0.8	3.98	−5.36	1925.1
20	10.8 ± 0.7	7.5 ± 1.3	12.1 ± 1.9	13.9 ± 1.8	3.24	−4.48	1522.1
21	9.2 ± 1.0	**3.9 ± 1.9** * (−57.6%)	8.7 ± 1.0	11.5 ± 1.3	5.16	−6.42	1665.0
22	10.8 ± 0.7	9.4 ± 2.1	12.1 ± 1.9	14.1 ± 1.1	5.16	−6.73	1370.8
23	11.3 ± 2.4	6.4 ± 1.5	9.8 ± 1.1	**14.1 ± 1.0** * (+43.9%)	4.10	−5.62	988.7
24	9.2 ± 1.0	8.1 ± 1.8	8.7 ± 1.0	9.1 ± 0.6	4.50	−4.61	1817.1
25	10.8 ± 0.7	9.8 ± 1.2	12.1 ± 1.9	18.3 ± 3.9	5.03	−5.98	2298.4
26	11.3 ± 2.4	8.3 ± 1.8	9.8 ± 1.1	**13.9 ± 0.8** * (+41.8%)	3.77	−4.11	1646.7
Sodium diclofenac	11.8 ± 0.5	**4.2 ± 0.8** * (−64.4%)	10.5 ± 1.4	**13.2 ± 1.4** * (+25.7%)	—	—	—

Notes: N is the number of writhings, τ represents the latent period between the animal's placement on the hot plate and the first observed nociceptive response (either paw licking or jumping). [a] Inhibition of pain response (IPR) = 100%•(Kcontrol − Kexp)/Kcontrol. [b] Protection P (%) = 100%•(Kexp − Kcontrol)/Kcontrol. *p* is the criterion for the presence of statistically significant differences in data compared to the control group: * $p < 0.05$, ** $p < 0.01$, *** $p < 0.001$.

The compounds **20** and **23** showed a nonsignificant trend for a lower number of acetic acid-induced writhings ($p = 0.09$ for both compounds). QPlogPo/w, predicted octanol/water partition coefficient; QPlogS, predicted aqueous solubility (log mol/L);

QPPCaco, predicted Caco-2 permeability (nm/s). Additional QikProp descriptors are provided in Table S1 (Supporting Information). For acridoneacetic acid, the Epik state with State Penalty = 0.0000 is shown.

Neither acridoneacetic acid nor Cycloferon® exhibited activity in either test, indicating a lack of analgesic effect. However, some cridanimod–monoterpene conjugates exhibited analgesic activity in at least one assay. Among the agents containing an amide substituent, compounds **17** and **19** significantly decreased the number of acetic acid-induced writhings (−38.9% and −63.7%, respectively), whereas compound **14** demonstrated analgesic activity on the hot plate (+62.1%). In addition, compound **20** tended to lower the number of acetic acid-induced writhings ($p = 0.09$). Among the agents containing an acylhydrazone fragment, compound **21** exhibited significant analgesic activity in the acetic acid-induced writhing test (−57.6%), and compound **23** showed a trend toward a lower number of writhings ($p = 0.09$). Moreover, compound **23** significantly increased the latency period on the hot plate (+43.9%). Among the esters, only compound **26** demonstrated significant analgesic activity in the hot plate test (+41.8%). The data are shown graphically in Figure 1.

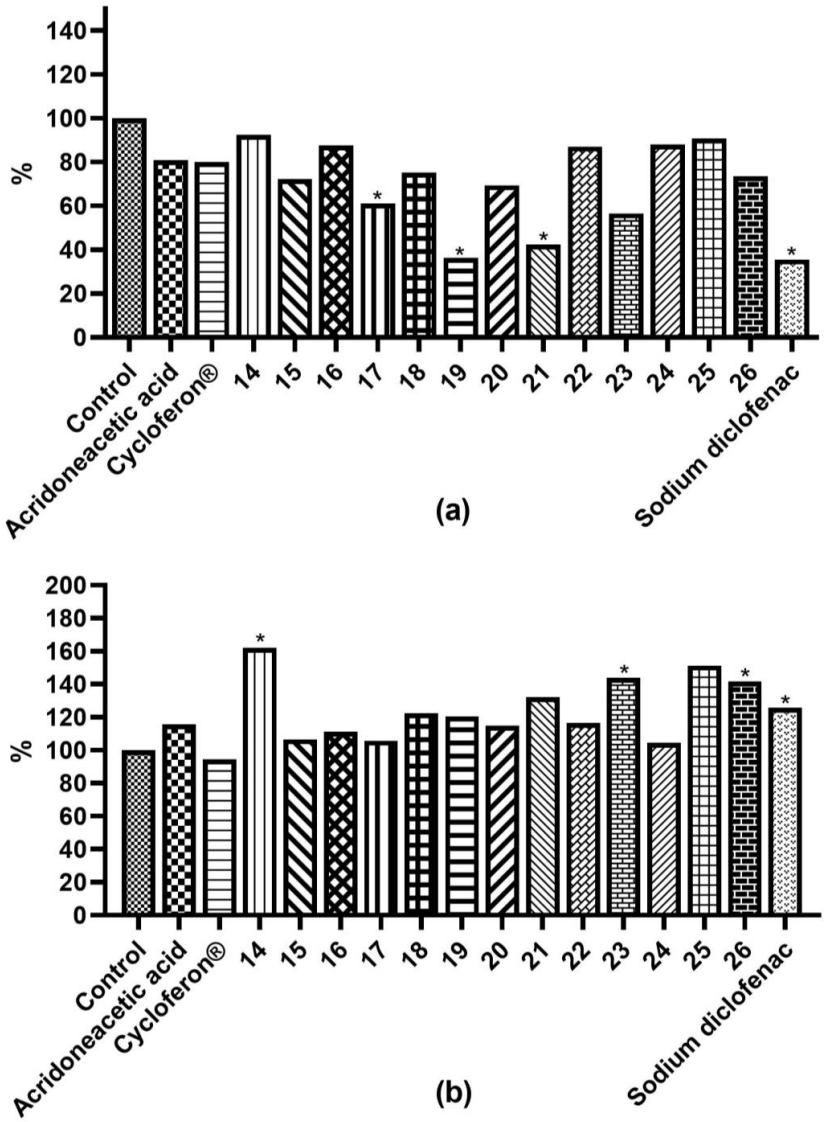

Figure 1. (**a**) Inhibition of pain response (IPR) in the acetic acid-induced writhing; (**b**) Protection (P) in the hot plate test. p is the criterion for the presence of statistically significant differences in data compared to the control group: * $p < 0.05$. Data are presented as a percentage of control, which was set to 100%.

Based on the obtained data, the following lead compounds can be identified: amide **19**, which was comparable to the reference drug diclofenac in the writhing test (−63.7% vs. −64.4%), and acylhydrazone **23**, which outperformed diclofenac in the hot plate test (+43.9% vs. +25.7%). Taken together, these findings indicate that derivatization of acridoneacetic acid may represent a viable approach to the development of new analgesic agents.

3.3. In Silico Physicochemical and ADME Profile

QikProp predictions indicated that conjugation increased lipophilicity and predicted intestinal permeability relative to acridoneacetic acid, while reducing predicted aqueous solubility (Table 2). For the conjugates, QPlogPo/w ranged from 3.039 to 5.163 and QPPCaco from 988.7 to 2298.4 nm/s, whereas QPlogS ranged from −4.114 to −6.728. Acridoneacetic acid showed QPlogPo/w = 2.211, QPPCaco = 132.958 nm/s, and QPlogS = −2.537.

All conjugates were predicted to have high oral absorption, although these in silico values should not be interpreted as experimentally determined bioavailability. Compounds **21**, **22**, and **25** showed one Lipinski Rule-of-Five violation and were among the most lipophilic derivatives. The full physicochemical profile, including the alternative protonation state of acridoneacetic acid, is provided in Table S1 (Supporting Information).

The calculated descriptors do not, by themselves, explain analgesic potency. For example, the strong activity of amide **19** in the writhing test and acylhydrazone **23** in the hot plate test cannot be reduced to a single logP or permeability value. Nevertheless, both compounds combine high predicted Caco-2 permeability with no Rule-of-Five violations, while avoiding the highest lipophilicity observed for **21**, **22**, and **25**. The in silico data therefore complement, rather than replace, the structure–activity analysis and support further optimization of the active conjugates with particular attention to the balance between permeability and aqueous solubility.

4. Conclusions

In this study, we explored the previously untapped analgesic potential of cridanimod (acridoneacetic acid) through molecular hybridization with bornane-type monoterpenoid fragments. A focused library of thirteen conjugates—seven amides, three acylhydrazones, and three esters—was assembled using two complementary protocols identified by systematic screening of seven activation strategies: EDCI/DMAP-mediated coupling for the amides and acylhydrazones and CDI/DBU-promoted esterification for the sterically hindered bornane alcohols. In vivo evaluation in the acetic acid writhing and hot plate tests revealed a clear contrast: whereas the parent acridoneacetic acid and its meglumine salt Cycloferon® were devoid of analgesic activity, six of the thirteen conjugates were significantly active ($p < 0.05$) in at least one model, with two distinct leads emerging—the amide 19, which matched the reference NSAID diclofenac in the writhing test (−63.7% vs. −64.4%), and the acylhydrazone **23**, which surpassed diclofenac in the hot plate test (+43.9% vs. +25.7%).

These findings demonstrate that conjugation transforms an analgesically inactive immunomodulator into derivatives that match or exceed a standard NSAID at the same oral dose, while the divergent activity profiles across the structural subclasses suggest that the linker type and monoterpene fragment together modulate the balance between peripheral and central antinociceptive mechanisms. Acridoneacetic acid thus represents a viable and largely unexplored scaffold for analgesic drug design, and further studies directed at elucidating the underlying mechanisms of action, refining the structure–activity relationships, and assessing the safety and pharmacokinetic profiles of the lead compounds are currently underway.

Supplementary Materials: The following supporting information can be downloaded at: https://www.mdpi.com/article/10.3390/scipharm94030063/s1.

Author Contributions: Conceptualization, D.D.A., O.I.Y. and K.S.K.; methodology, D.D.A., A.Y.F., A.V.P., O.I.Y., K.S.K., M.V.K. and T.G.T.; investigation, D.D.A., S.A.T. and A.A.S.; resources, A.V.P., M.V.K. and T.G.T.; data curation, D.D.A., A.Y.F. and S.A.T.; formal analysis, D.D.A., A.Y.F., S.A.T., A.A.S. and A.Y.P.; writing—original draft, D.D.A., A.Y.F., O.I.Y. and A.V.P.; writing—review and editing, K.S.K., O.I.Y. and A.Y.P.; validation, O.I.Y.; supervision, A.V.P., K.S.K., M.V.K., T.G.T. and N.F.S.; project administration, K.S.K.; funding acquisition, O.I.Y. and N.F.S. All authors have read and agreed to the published version of the manuscript.

Funding: This work was financially supported by the Russian Science Foundation and the Government of the Novosibirsk region (Project № 26-23-20046).

Institutional Review Board Statement: The study was approved by the Bioethics Commission of the Laboratory of Pharmacological Research, N.N. Vorozhtsov Novosibirsk Institute of Organic Chemistry, SB RAS (protocol code R-14-2026-04-01 and date of approval: 1 April 2026).

Informed Consent Statement: Not applicable.

Data Availability Statement: The original contributions presented in this study are included in the article. Further inquiries can be directed to the corresponding author.

Acknowledgments: The authors would like to acknowledge the Multi-Access Chemical Service Centre SB RAS for spectral and analytical measurements. The authors also gratefully acknowledge Polysan for providing acridoneacetic acid.

Conflicts of Interest: The authors declare no conflicts of interest.

References

1. Cohen, S.P.; Vase, L.; Hooten, W.M. Chronic Pain: An Update on Burden, Best Practices, and New Advances. *Lancet* **2021**, *397*, 2082–2097. [CrossRef] [PubMed]
2. Domper Arnal, M.-J.; Hijos-Mallada, G.; Lanas, A. Gastrointestinal and Cardiovascular Adverse Events Associated with NSAIDs. *Expert Opin. Drug Saf.* **2022**, *21*, 373–384. [CrossRef] [PubMed]
3. Coxib and traditional NSAID Trialists' (CNT) Collaboration; Bhala, N.; Emberson, J.; Merhi, A.; Abramson, S.; Arber, N.; A Baron, J.; Bombardier, C.; Cannon, C.; E Farkouh, M.; et al. Vascular and Upper Gastrointestinal Effects of Non-Steroidal Anti-Inflammatory Drugs: Meta-Analyses of Individual Participant Data from Randomised Trials. *Lancet* **2013**, *382*, 769–779. [CrossRef] [PubMed]
4. Kovalenko, A.L.; Romantsev, M.G.; Ershov, F.I. Acridonacetic acid: Pharmacological properties and clinical use. *Zh. Mikrobiol. Epidemiol. Immunobiol.* **2000**, *5*, 103–108.
5. Keyer, V.; Syzdykova, L.; Zauatbayeva, G.; Zhulikeyeva, A.; Ramanculov, Y.; Shustov, A.V.; Shulgau, Z. Tilorone and Cridanimod Protect Mice and Show Antiviral Activity in Rats despite Absence of the Interferon-Inducing Effect in Rats. *Pharmaceuticals* **2022**, *15*, 617. [CrossRef] [PubMed]
6. Mazina, N.K.; Sheshunov, I.V.; Mazin, P.V.; Mazin, V.P.; Kovalenko, A.L.; Zaplutanov, V.A. Clinical Efficacy of the Immunomodulatory Agent Cycloferon (Tablets) in Viral Respiratory Infections: Results of a Systematic Review and Meta-Analysis. *Ter. Arkh.* **2017**, *89*, 84–92. [CrossRef] [PubMed]
7. Plotnikova, M.A.; Klotchenko, S.A.; Kiselev, A.A.; Gorshkov, A.N.; Shurygina, A.-P.S.; Vasilyev, K.A.; Uciechowska-Kaczmarzyk, U.; Samsonov, S.A.; Kovalenko, A.L.; Vasin, A.V. Meglumine Acridone Acetate, the Ionic Salt of CMA and N-Methylglucamine, Induces Apoptosis in Human PBMCs via the Mitochondrial Pathway. *Sci. Rep.* **2019**, *9*, 18240. [CrossRef] [PubMed]
8. Cavlar, T.; Deimling, T.; Ablasser, A.; Hopfner, K.; Hornung, V. Species-specific Detection of the Antiviral Small-molecule Compound CMA by STING. *EMBO J.* **2013**, *32*, 1440–1450. [CrossRef] [PubMed]
9. Zhurinov, M.Z.; Miftakhova, A.F.; Keyer, V.; Shulgau, Z.T.; Solodova, E.V.; Kalykberdiyev, M.K.; Abilmagzhanov, A.Z.; Talgatov, E.T.; Ait, S.; Shustov, A.V.; et al. Extracts and Other Therapeutics against SARS-CoV-2 in Central Eurasia: Available but Overlooked. *Molecules* **2023**, *28*, 6142. [CrossRef] [PubMed]
10. Salakhutdinov, N.F.; Volcho, K.P.; Yarovaya, O.I. Monoterpenes as a Renewable Source of Biologically Active Compounds. *Pure Appl. Chem.* **2017**, *89*, 1105–1117. [CrossRef]
11. Zielińska-Błajet, M.; Feder-Kubis, J. Monoterpenes and Their Derivatives—Recent Development in Biological and Medical Applications. *Int. J. Mol. Sci.* **2020**, *21*, 7078. [CrossRef] [PubMed]

12. Sokolova, A.S.; Kovaleva, K.S.; Kuranov, S.O.; Bormotov, N.I.; Borisevich, S.S.; Zhukovets, A.A.; Yarovaya, O.I.; Serova, O.A.; Nawrozkij, M.B.; Vernigora, A.A.; et al. Design, Synthesis, and Biological Evaluation of (+)-Camphor- and (−)-Fenchone-Based Derivatives as Potent Orthopoxvirus Inhibitors. *ChemMedChem* **2022**, *17*, e202100771. [CrossRef] [PubMed]
13. Almeida, J.R.G.D.S.; Souza, G.R.; Silva, J.C.; Saraiva, S.R.G.D.L.; Júnior, R.G.D.O.; Quintans, J.D.S.S.; Barreto, R.D.S.S.; Bonjardim, L.R.; Cavalcanti, S.C.D.H.; Junior, L.J.Q. Borneol, a Bicyclic Monoterpene Alcohol, Reduces Nociceptive Behavior and Inflammatory Response in Mice. *Sci. World J.* **2013**, *2013*, 808460. [CrossRef] [PubMed]
14. Wang, X.; Guo, C.; Shao, J.; Zou, X.; Xing, S.; Xu, C.L.; Zhao, Q.; Wu, Y.; Sun, C.; Chen, Y.; et al. Small Molecule-Drug Conjugates: An Emerging Drug Design Strategy for Targeted Therapeutics. *J. Med. Chem.* **2025**, *68*, 24759–24784. [CrossRef] [PubMed]
15. De Sena Murteira Pinheiro, P.; Franco, L.S.; Montagnoli, T.L.; Fraga, C.A.M. Molecular Hybridization: A Powerful Tool for Multitarget Drug Discovery. *Expert Opin. Drug Discov.* **2024**, *19*, 451–470. [CrossRef] [PubMed]
16. Eddy, N.B.; Leimbach, D. Synthetic Analgesics. II. Dithienylbutenyl- and Dithienylbutylamines. *J. Pharmacol. Exp. Ther.* **1953**, *107*, 385–393. [CrossRef]
17. Morozova, E.A.; Tolstikova, T.G.; Bolkunov, A.V.; Dolgikh, M.P.; Shul'ts, E.E. Analgesic Properties of New Pyrrolidinomorphinane Derivatives: Revealing Potential Pathways. *Nat. Prod. Commun.* **2008**, *3*, 1934578X0800301008. [CrossRef]
18. Koster, R.; Anderson, M.; de Beer, E.J. Acetic Acid for Analgesic Screening. *Fed. Proc.* **1959**, *18*, 412–414.
19. Tishchenko, S.A.; Sokolova, A.S.; Yarovaya, O.I.; Krasnov, V.I.; Shtro, A.A.; Galochkina, A.V.; Klabukov, A.M.; Razgulyaeva, D.N.; Salakhutdinov, N.F. Synthesis of Secondary Amines of Bornylamine and Isobornylamine Containing a Saturated N-Heterocycle and Study of Their Antiviral Activity against Respiratory Syncytial Virus. *Russ. J. Gen. Chem.* **2025**, *95*, 79–87. [CrossRef]
20. Tishchenko, S.A.; Sokolova, A.S.; Arbuzova, M.A.; Selyutina, O.Y.; Tsypyshev, D.O.; Yarovaya, O.I.; Arkhipov, S.G.; Salakhutdinov, N.F. Synthesis and a Kinetic Study of the Reactivity of 1-Amino-7,7-dimethylbicyclo[2.2.1]Heptan-2-one in Alkylation Reactions with Structurally Similar Amines. *ChemistrySelect* **2025**, *10*, e05689. [CrossRef]
21. Kokova, V.; Apostolova, E. Experimental Models and Tests for Nociceptive and Neuropathic Pain Evaluation. *Knowl.-Int. J.* **2022**, *51*, 609–614.